

Image denoising via K-SVD with primal-dual active set algorithm

Quan Xiao

Canhong Wen*

Zirui Yan

Department of Statistics and Finance

School of Management

University of Science and Technology of China

xq2016@mail.ustc.edu.cn

wench@ustc.edu.cn

zincrain@mail.ustc.edu.cn

Abstract

K-SVD algorithm has been successfully applied to image denoising tasks dozens of years but the big bottleneck in speed and accuracy still needs attention to break. For the sparse coding stage in K-SVD, which involves ℓ_0 constraint, prevailing methods usually seek approximate solutions greedily but are less effective once the noise level is high. The alternative ℓ_1 optimization is proved to be powerful than ℓ_0 , however, the time consumption prevents it from the implementation. In this paper, we propose a new K-SVD framework called K-SVD_P by applying the Primal-dual active set (PDAS) algorithm to it. Different from the greedy algorithms based K-SVD, the K-SVD_P algorithm develops a selection strategy motivated by KKT (Karush-Kuhn-Tucker) condition and yields to an efficient update in the sparse coding stage. Since the K-SVD_P algorithm seeks for an equivalent solution to the dual problem iteratively with simple explicit expression in this denoising problem, speed and quality of denoising can be reached simultaneously. Experiments are carried out and demonstrate the comparable denoising performance of our K-SVD_P with state-of-the-art methods.

1. Introduction

Image denoising problem is primal in various regions such as image processing and computer visions. The goal of denoising is to remove noise from noisy images and retain the actual signal as precisely as possible. Many methods based on sparse representation have been proposed to accomplish this goal in the past few decades [26, 7, 21, 23, 15, 3]. K-means singular value decomposition (K-SVD) is one of the typical works among these models. It is an iterative patch-based procedure aiming at finding an optimal linear combination of an overcomplete dictionary to best describe the image. The solid theoretical

foundations [19] and adaptability make it boost for dozens of years. It can be divided into two stages, one is the dictionary learning stage and the other is the sparse coding stage. Some recent researches have been seeking for highly efficient ways to make a breakthrough, but these modifications mostly are taken on the dictionary learning stage [6, 10].

In fact, sparse coding is an optimization problem and ℓ_1 optimization [27, 32, 8] is proved more powerful in solving denoising problems when the noise level is high [11]. However, taking time consumption into consideration, the image denoising area always prefers to approximate the ℓ_0 solutions using greedy algorithms instead [9] and treats it as benchmark of K-SVD [2, 9, 26, 19, 18, 1]. Recently, Liu *et al.* [14] apply the Mixed Integer quadratic programming (MIQP) in the sparse coding stage which yields the global optimal solution, but it also takes a long time. Thus, a tradeoff between computational efficiency and denoising performance in high noise conditions is needed.

In this paper, primal-dual active set algorithm (PDAS) is applied to the sparse coding stage in the K-SVD framework, and the new framework is called K-SVD_P. PDAS algorithm is first proposed by Ito and Kunisch in 2013 [12] and then generalized and implemented by Wen, Zhang *et al.* in 2017 [31]. By using the KKT condition and introducing the primal-dual variables, this NP-hard problem [16] can be switched to a restricted linear regression model which can be solved explicitly. We demonstrate the feasibility of this new scheme and compare it with the existing K-SVD models achieved by orthogonal matching pursuit (OMP) algorithm [28, 29], a typical ℓ_0 greedy algorithm, and Basis pursuit Denoising (BPDN) algorithm (also known as LASSO in statistics) [27, 24], a classic ℓ_1 optimization algorithm, in experiment. The potential of our method will be verified both theoretically and experimentally.

These are our major contributions:

- We successfully build a new K-SVD_P framework by applying the PDAS algorithm to sparse coding stage and reach an explicit expression in this special case;

*Canhong Wen is the corresponding author.

- Comparison with the representative algorithms OMP and BPDN are taken both theoretically and empirically;
- The results demonstrate the proposed K-SVD_P is competitive when the noise is low and has superior performance in highly noisy images compared to the state-of-art methods.

The rest of the paper is organized as follows. In Section 2, we state the image denoising problem and introduce the K-SVD framework. In Section 3, K-SVD_P is proposed and theoretical analysis is described. In Section 4, experiments in image denoising are carried out and the results are showed. In Section 5, we arrive at the conclusion and mention the possible future work.

2. Problem statement and K-SVD framework

Image denoising problem can be described as $\beta = \alpha + \epsilon$, where α is the original noise-free image, ϵ is the added random Gaussian white noise, and β denotes the noisy image. Our target is to move ϵ from given β and obtain the real image α .

In order to achieve this, sparse representation model first searches for the principal component of the image called dictionary by extracting sparse elements patch by patch in β , and then treats the residual as noise ϵ and throw it out, and finally reconstruct the image α based on the sparse representation of the selected image elements. In this paper, we only focus on the first phase of the above procedure which the K-SVD algorithm is designed for and the other details can be found in [9].

Considering a signal matrix $Y = \{y_j\}_{j=1}^p \in \mathbb{R}^{n \times p}$ with p original signals, a dictionary $D = \{d_j\}_{j=1}^K \in \mathbb{R}^{n \times K}$ with K prototype signal-atoms and sparse representation $X = \{x_j\}_{j=1}^p \in \mathbb{R}^{K \times p}$ with p solutions x_j of corresponding y_j . The optimization object can be formulated as:

$$\arg \min_{D, X} \{ \|Y - DX\|_F^2 \} \quad s.t. \|x_i\|_0 \leq T_0, i = 1, 2, \dots, p \quad (1)$$

where T_0 is the sparsity level, *i.e.* ℓ_0 -norm counting the number of nonzero elements in a vector, and $\|Y - DX\|_F^2 = \sum \|y_i - Dx_i\|_2^2$, *i.e.* the the Frobenius Norm of matrix $Y - DX$.

K-SVD algorithm consists of dictionary learning and sparse coding stage. The dictionary learning stage is to update the dictionary and corresponding coefficient with given X , and the sparse coding stage deals with finding the sparse coefficient x_i to each y_i with known dictionary D . To simplify the formula at sparse coding stage, let y and x denote y_i and x_i , the target is as follows:

$$\hat{x} = \arg \min \|y - Dx\|_2^2 \quad s.t. \|x\|_0 \leq T_0. \quad (2)$$

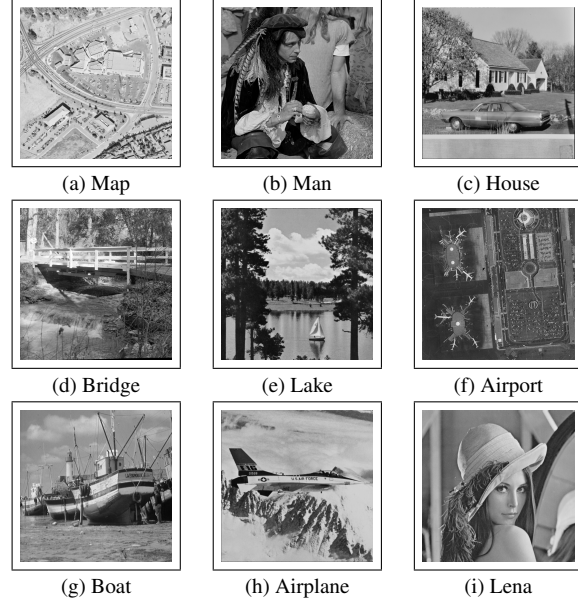


Figure 1. Chosen images from USC-SIPI Image Database

The dictionary learning stage is generally solved by applying Single-Value Decomposition (SVD) to nonzero sub-matrix of each $E_i = Y - \sum_{j \neq i} d_j x_{(j)}$, where $x_{(j)}$ denotes the j -th row of X since the first column of singular value vector contains the highest proportion of information. That is, to extract the first column of the left singular value vector to update atoms column and treat the first column of the right singular value vector as the corresponding coefficient column. The details can be found in [2].

While the dictionary updating stage generates a convex optimization problem, the sparse coding stage with ℓ_0 -norm constraint is more challenging.

3. Proposed pursuit algorithm

Since the problem in (2) is NP-hard problem[16], prevailing algorithms usually search for approximate solutions by greedy algorithms (*e.g.* Matching pursuit [4], Orthogonal matching pursuit [28]). However, most of these approaches suffer from insufficient precision in high noise level [13]. A remedy is turning to solve ℓ_1 optimization (*e.g.* Basis pursuit[5], Basis pursuit Denoising [27, 24]) which has promising accuracy equivalently [11], but the computational expense makes it infeasible in large-scale denoising problems. This really obstructs the development of the K-SVD framework in image denoising, since at least thousands of patches are in the process even if for the small 124×124 image.

In this section, we plug a special case of the PDAS algorithm, proposed by Wen *et al.* [31] who derived KKT condition for general convex loss functions, in the K-SVD_P sparse coding stage. The goal of this section is to derive

an explicit expression in the denoising problem, and then discuss the connection with existing approaches.

3.1. The K-SVD_P sparse coding stage

It's known that solution to (2) is necessarily a coordinate-wise minimizer. So, let $x^\diamond = (x_1^\diamond, \dots, x_K^\diamond)$ be the coordinate-wise minimizer, *i.e.* each x_j^\diamond is minimizer in its coordinate. A simple observation is that:

$$\begin{aligned} \|y - Dx\|_2^2 &= \sum_{i=1}^n (y_i - \sum_{q=1}^K D_{iq}x_q)^2 \\ &= \sum_{i=1}^n (y_i - \sum_{q \neq j} D_{iq}x_q - D_{ij}x_j)^2 \\ &= \sum_{i=1}^n (y_i - \sum_{q \neq j} D_{iq}x_q)^2 \\ &\quad - 2 \sum_{i=1}^n (y_i - \sum_{q \neq j} D_{iq}x_q) D_{ij}x_j + \sum_{i=1}^n D_{ij}^2 x_j^2 \\ &= \sum_{i=1}^n (y_i - \sum_{q \neq j} D_{iq}x_q)^2 \\ &\quad - 2 \sum_{i=1}^n (y_i - \sum_{q \neq j} D_{iq}x_q) D_{ij}x_j + x_j^2 \end{aligned} \quad (3)$$

where last equation is arrived since dictionary D is normalized.

In order to find coordinate-wise minimizer, we define a quadratic function respective to t in each coordinate j which freezes x in the other coordinates to their optimal choices:

$$l_j(t) = \sum_{i=1}^n (y_i - \sum_{q \neq j} D_{iq}x_q^\diamond)^2 - 2 \sum_{i=1}^n (y_i - \sum_{q \neq j} D_{iq}x_q^\diamond) D_{ij}t + t^2 \quad (4)$$

Then $l_j(t)$ achieve global minimum if and only if $t_j^* = \sum_{i=1}^n (y_i - \sum_{q \neq j} D_{iq}x_q^\diamond) D_{ij}$. For simplicity, let d_j denotes the j -th column of D , and define $g_j^\diamond = (y - Dx^\diamond)^\circ d_j$. In this way, $t_j^* = x_j^\diamond + g_j^\diamond$. It's natural to define a sacrifice of $l_j(t)$ if we push t_j^* from desirable value $x_j^\diamond + g_j^\diamond$ to zero, and that is:

$$h_j = \frac{1}{2} (x_j^\diamond + g_j^\diamond)^2 \quad (5)$$

We tend to set those scarify less to zero. *i.e.*

$$x_j^\diamond = \begin{cases} x_j^\diamond + g_j^\diamond, & \text{if } h_j \geq h_{[T_0]} \\ 0, & \text{else,} \end{cases} \quad \text{for } j = 1, \dots, K, \quad (6)$$

Actually, these are the KKT conditions of x^\diamond proved in [?]. So x^\diamond is the solution to (2) if and only if it satisfies the above conditions. We can tell from (6) that if $x_j \neq 0$, then x_j is the optimal value and $g_j = 0$, and if not, $g_j \neq 0$ as defined. This observation indicates x_j and g_j have complementary supports and we can treat them as a pair of primal-dual variables. Then, searching for a solution to (2) is equal to finding the best dual variable g_j . Let \mathcal{A} be the indicator set of

nonzero elements in coefficient x and $\mathcal{I} = (\mathcal{A})^c$. Then we arrive at:

$$\begin{cases} x_{\mathcal{I}} = 0, \\ g_{\mathcal{A}} = 0, \\ x_{\mathcal{A}} = (D'_{\mathcal{A}} D_{\mathcal{A}})^{-1} D'_{\mathcal{A}} y, \\ g_{\mathcal{I}} = (y - Dx)^T D_{\mathcal{I}}, \\ h_{\mathcal{I}} = \frac{1}{2} (g_{\mathcal{I}})^2, \\ h_{\mathcal{A}} = \frac{1}{2} (x_{\mathcal{A}})^2 \end{cases} \quad (7)$$

and

$$\mathcal{A} = \{j : h_j \geq h_{[k]}\}, \quad \mathcal{I} = \{j : h_j < h_{[k]}\} \quad (8)$$

where $h_{[1]} \geq h_{[2]} \geq \dots \geq h_{[K]}$ denotes the decreasing permutation of h . We solve this problem iteratively and reach the pursuit algorithm in Algorithm 1.

Algorithm 1: Sparse coding algorithm in K-SVD_P

Input: Signal y , fixed dictionary $D \in \mathbb{R}^{n \times K}$, the maximum number of iterations R and ℓ_0 -norm constraint T_0

Output: Sparse representation x

Initialization: randomly set \mathcal{A}^0 be a T_0 subset of $\{1, \dots, K\}$ and $\mathcal{I}^0 = (\mathcal{A}^0)^c$;

for $r \in \{0, 1, \dots, R\}$ **do**

• Compute $x_{\mathcal{I}}^r, x_{\mathcal{A}}^r, g_{\mathcal{I}}^r, g_{\mathcal{A}}^r, h_{\mathcal{I}}^r, h_{\mathcal{A}}^r$ by equation (6) where $\mathcal{A} = \mathcal{A}^r$;

• Sort h_j by $h_{[1]}^r \geq h_{[2]}^r \geq \dots \geq h_{[K]}^r$;

• Update the active and inactive sets by

$$\mathcal{A}^{r+1} = \{j : h_j^r \geq h_{[T_0]}^r\},$$

$$\mathcal{I}^{r+1} = \{j : h_j^r < h_{[T_0]}^r\}$$

• If $\mathcal{A}^{r+1} = \mathcal{A}^r$, then stop; else $r = r + 1$ and return to steps above.

end

3.2. Comparison with existing approach

3.2.1 Comparison to greedy algorithms

In this part, a theoretical comparison to the representative of greedy algorithm Orthogonal matching pursuit algorithm (OMP) [28] is given. OMP algorithm is an iterative method. Let P_i be the indicator set of dictionary atoms have been selected until i -th step and R_i be the residual in i -th step, *i.e.* $R_i = y - Dx^{(i)}$ where $x^{(i)}$ denotes the sparse coefficient x in i -th step. At $(i+1)$ -th step, one atom d_j that is most correlated to the residual R_i is selected by maximizing $|\langle d_j, R_i \rangle|$ which is same as dual variables $g_j = (y - Dx)' d_j$ defined in the K-SVD_P algorithm. Then, in order to keep new residual orthogonal to selected dictionary atoms, the OMP algorithm estimates the nonzero elements of $x^{(i+1)}$ and computes residual R_{i+1} by applying

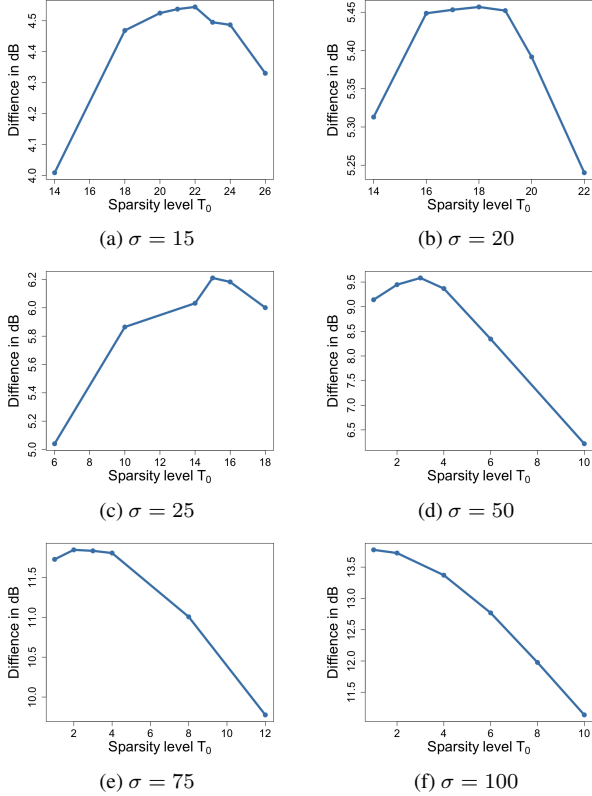


Figure 2. PSNR of K-SVD_P versus sparsity levels T_0 with $\sigma = 15, 20, 25, 50, 75, 100$

least squares to y on dictionary atoms have been selected already, *i.e.* $x^{(i+1)} = (D'_{P_i} D_{P_i})^{-1} D'_{P_i} y$. After several iterations, this algorithm will converge.

However, from equation (5), we can tell that the K-SVD_P algorithm updates T_0 atoms in the active set each time based on h_j which collects information both in primal and dual variables iteratively. This procedure will gather more information in each step, which accelerates the convergence and improves the denoising performance.

3.2.2 Comparison with ℓ_1 denoising

Since ℓ_1 -norm is the closest convex function to ℓ_0 -norm, alternative methods seek for ℓ_1 constraint solution of problem (1). By transforming the ℓ_0 -norm into ℓ_1 -norm and formulating the Lagrangian function, the problem is changed to basis pursuit denoising (BPDN) problem, which is also known as LASSO [27] in statistics.

$$\hat{x}(\lambda) = \arg \min \|y - Dx\|_2^2 + \lambda \|x\|_1 \quad (9)$$

Recently, Hastie *et al.* (2017) showed that neither best subset selection (2) nor LASSO (9) dominates in terms of accuracy, with best subset selection performs better in low noisy

σ	15	20	25	50	75	100
T_0	20	20	15	2	2	2

Table 1. Chosen sparsity level T_0 in $\sigma = 15, 20, 25, 50, 75, 100$

conditions and LASSO better in highly noisy images[11]. This tolerance of high noise partly thanks to the shrinkage in LASSO, since the fitted variables from LASSO are continuous functions of x . [32] Best subset selection will hit discontinuous points when x is moving from \mathcal{I} to \mathcal{A} or from \mathcal{A} to \mathcal{I} which makes them susceptible to high noise. However, the K-SVD_P based on best subset selection is still attractive since its time complexity is far less than LASSO as shown in the next section. As is said in [28], if there is an approximant holding of good quality, there is no need to waste time in finding another closer solution.

4. Experiment

4.1. Design and Parameter setting

We select 9 images of size 512×512 , as shown in Figure 1, from classic USC-SIPI Image Database[17] to compare the image denoising performance of the K-SVD_P with the OMP and the BPDN-based K-SVD scheme.

For similarity, we set the number of iteration of K-SVD to 10 for all pursuit algorithms. For each image, $p = 500$ overlapping patches of size $n = 8 \times 8$ are extracted to learn the dictionary D of size 64×256 as suggested [9]. The experiment is repeated for noise levels $\sigma = 15, 20, 25, 50, 75, 100$. Note that the last three are the high noise level benchmarks according to [9]. In order to select the optimal sparsity level T_0 at different noise levels for K-SVD_P, we start with the noisy Man image for the experiment. In each sparsity level for each σ , we compute the peak signal-to-noise ratio (PSNR) of the restored image. The PSNR of two images x and y is defined as (10). The results are presented in Figure 2. Based on the results, the optimal sparsity levels are chosen in Table 1.

$$\text{PSNR} = -10 \log \frac{\|x - y\|^2}{255^2} \quad (10)$$

σ	15	20	25	50	75	100
BPDN	1178.91	1177.59	1180.31	-	-	-
OMP	78.04	80.82	83.20	78.76	79.33	78.37
K-SVD _P	93.29	96.19	84.28	58.93	59.47	61.56

Table 2. Reconstruction time(s) with $\sigma = 15, 20, 25, 50, 75, 100$

For the OMP algorithm, we run the supplementary code provided by [9] and use the same method as we used for K-SVD_P to find its optimal sparsity levels. We choose the SpaSM toolbox [25] based on piece-wise solution path [22] to solve the LASSO problem in BPDN algorithm since it is faster than the popular glmnet package [20].

Figure	Map			Man			House		
$\sigma/PSNR$	BPDN	OMP	K-SVD _P	BPDN	OMP	K-SVD _P	BPDN	OMP	K-SVD _P
15/24.61	27.10	28.39	27.83	28.87	29.31	29.04	28.67	29.10	28.71
20/22.11	25.99	26.63	26.38	27.55	27.24	27.50	27.39	27.12	27.08
25/20.17	24.97	25.07	24.98	26.37	25.57	26.09	26.23	25.46	25.88
Figure	Bridge			Lake			Airport		
$\sigma/PSNR$	BPDN	OMP	K-SVD _P	BPDN	OMP	K-SVD _P	BPDN	OMP	K-SVD _P
15/24.61	26.72	27.82	27.34	28.74	29.04	28.71	29.14	29.55	29.41
20/22.11	25.81	26.26	26.15	27.40	27.05	27.15	27.64	27.32	27.58
25/20.17	24.95	24.87	24.99	26.28	25.45	26.14	26.45	25.62	26.48
Figure	Boat			Airplane			Lena		
$\sigma/PSNR$	BPDN	OMP	K-SVD _P	BPDN	OMP	K-SVD _P	BPDN	OMP	K-SVD _P
15/24.61	29.25	29.28	29.12	29.73	29.59	29.39	30.89	29.89	30.07
20/22.11	27.77	27.27	27.42	28.27	27.42	27.52	29.09	27.64	28.27
25/20.17	26.64	25.57	26.42	26.87	25.65	26.62	27.62	25.83	27.45

Table 3. Accuracy of the reconstruction PSNR(in dB) with $\sigma = 15, 20, 25$ (The higher, the better)

Figure	Map		Man		House		Birdge		Lake	
$\sigma/PSNR$	OMP	K-SVD _P	OMP	K-SVD _P	OMP	K-SVD _P	OMP	K-SVD _P	OMP	K-SVD _P
50/14.15	19.75	21.76	19.92	23.74	19.87	23.26	19.68	22.26	19.88	23.35
75/10.63	16.40	20.67	16.48	22.30	16.46	21.85	16.39	21.29	16.47	21.87
100/8.13	13.97	19.83	14.02	21.17	14.00	20.78	13.99	20.26	14.04	20.81
Figure	Airport		Boat		Airplane		Lena		Average	
$\sigma/PSNR$	OMP	K-SVD _P	OMP	K-SVD _P	OMP	K-SVD _P	OMP	K-SVD _P	OMP	K-SVD _P
50/14.15	19.90	23.85	19.96	24.13	19.96	24.03	19.99	25.67	19.88	23.56
75/10.63	16.48	22.48	16.48	22.61	16.49	22.26	16.54	23.87	16.47	22.13
100/8.13	14.03	21.34	14.02	21.36	14.04	21.11	14.06	22.41	14.02	21.01

Table 4. Accuracy of the reconstruction in terms of the PSNR(in dB) with $\sigma = 50, 75, 100$ (The best are highlighted in bold)

4.2. Reconstruction time

For $\sigma = 15, 20, 25$, we test the performance of three methods, BPDN, OMP and K-SVD_P, and run software in the Matlab[®] R2017b environment on the Macbook with 2.9 GHz Intel[®] Core[™] i5 processor and 8G memory. For each noise level, we record the average reconstruction time among different images since the time expense is stable when images change. For $\sigma = 50, 75, 100$, although BPDN may gain a bit higher quality, we need to abandon it since its time complexity is nearly 15 times that of the other two algorithms. This can be tell from Table 2. At the same time, we change to Matlab[®] R2019a online environment which is faster to test the other two. The reconstruction time results are shown in Table 2. From the result, we can conclude that proposed K-SVD_P framework is significant better than BPDN and is competitive to the OMP especially for images with high noise in terms of time.

4.3. PSNR comparison

Table 3 shows PSNR results in low noisy cases. We can tell that the reconstruction performance of BPDN is better when the noise level is relatively high but the margin of difference with K-SVD_P decreases when the noise level declines just as discussed in 3.2.2. The comparison between OMP and K-SVD_P is exactly the opposite. Considering the time consumption and the fact that almost all the previous K-SVD benchmarks choose OMP as pursuit algorithm [18, 1], so the next comparisons are only between OMP and K-SVD_P.

The high noise levels results of OMP and K-SVD_P are shown in Table 4. For all images, K-SVD_P outperforms OMP by a significant margin in high noise levels. In average, K-SVD_P improves 3.68, 5.66, 6.99dB at $\sigma = 50, 75, 100$ respectively. Figure 3 shows the difference of PSNR versus noise level for 9 images, and we can clearly see that K-SVD_P is markedly potential as the noise level increases. This result can be expected. From 3.2.1, we know

Figure	Map		Man		House		Birdge		Lake	
$\sigma/SSIM$	OMP	K-SVD _P	OMP	K-SVD _P	OMP	K-SVD _P	OMP	K-SVD _P	OMP	K-SVD _P
15/0.829	0.928	0.921	0.910	0.907	0.892	0.891	0.931	0.923	0.896	0.896
20/0.753	0.892	0.887	0.866	0.867	0.846	0.847	0.898	0.893	0.846	0.851
25/0.683	0.854	0.848	0.819	0.835	0.795	0.816	0.864	0.852	0.797	0.828
50/0.443	0.678	0.679	0.619	0.707	0.596	0.714	0.683	0.677	0.596	0.743
75/0.307	0.534	0.599	0.475	0.620	0.459	0.626	0.536	0.614	0.464	0.649
100/0.223	0.430	0.544	0.372	0.556	0.360	0.551	0.425	0.557	0.370	0.569
Figure	Airport		Boat		Airplane		Lena		Average	
$\sigma/SSIM$	OMP	K-SVD _P	OMP	K-SVD _P	OMP	K-SVD _P	OMP	K-SVD _P	OMP	K-SVD _P
15/0.829	0.897	0.893	0.897	0.895	0.874	0.878	0.881	0.889	0.901	0.899
20/0.753	0.850	0.848	0.847	0.847	0.818	0.828	0.827	0.839	0.854	0.856
25/0.683	0.800	0.810	0.795	0.819	0.759	0.800	0.769	0.821	0.806	0.825
50/0.443	0.585	0.664	0.579	0.711	0.544	0.743	0.541	0.754	0.602	0.710
75/0.307	0.434	0.574	0.432	0.621	0.414	0.635	0.395	0.660	0.460	0.622
100/0.223	0.333	0.509	0.333	0.540	0.331	0.554	0.304	0.575	0.362	0.551

Table 5. Accuracy of the reconstruction in terms of the SSIM with $\sigma = 15, 20, 25, 50, 75, 100$ (The best are highlighted in bold)

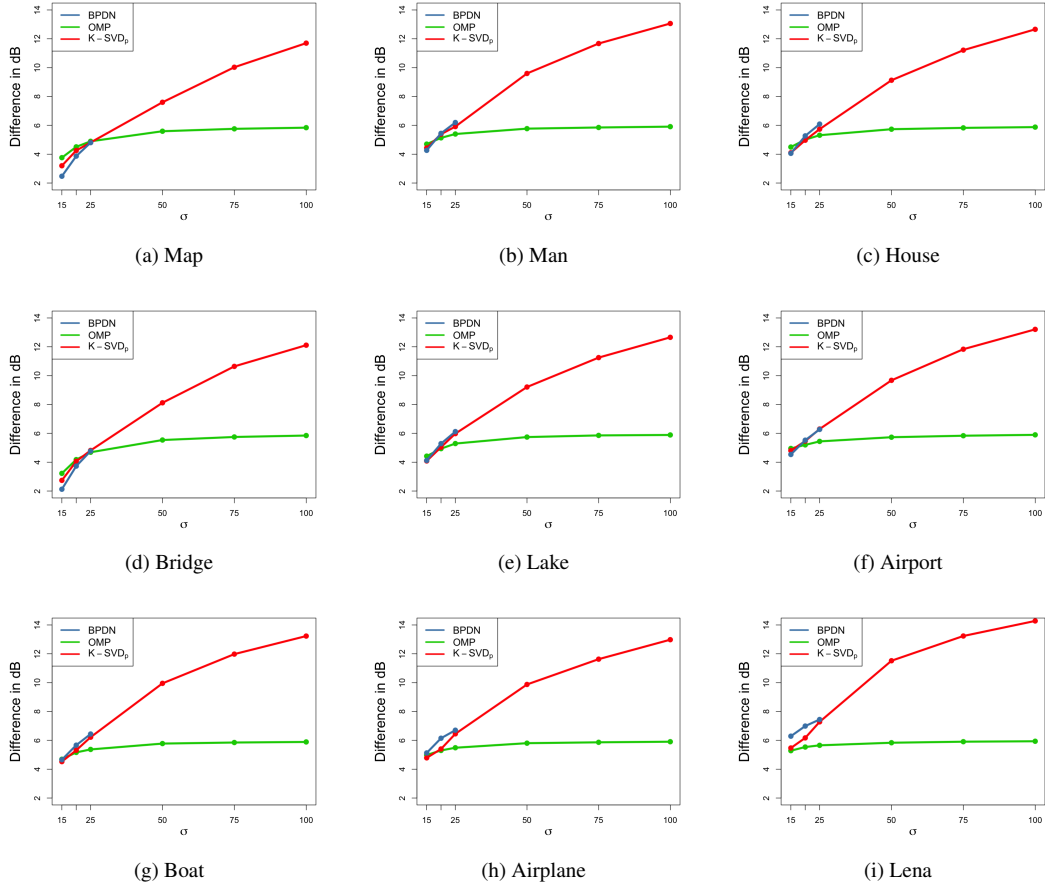


Figure 3. The difference of PSNR versus noise level of 9 images using different algorithms

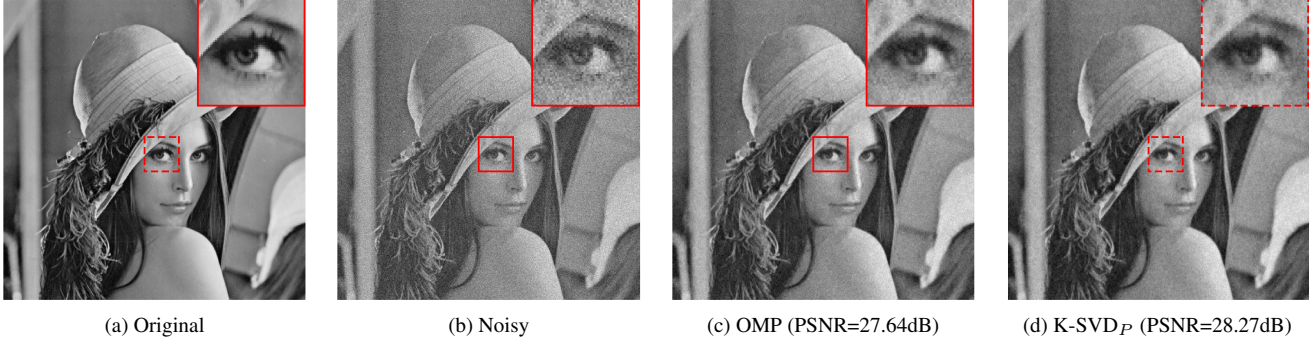


Figure 4. Denoising results in Lena, $\sigma = 20$

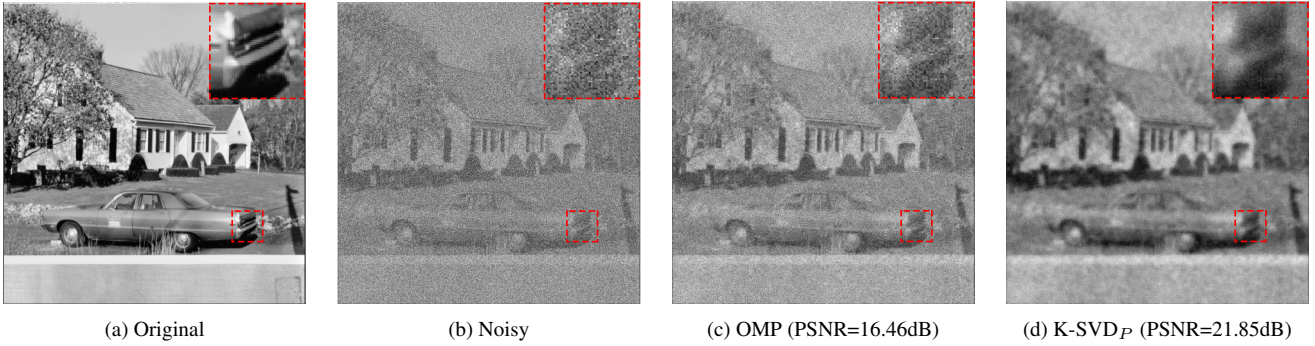


Figure 5. Denoising results in House, $\sigma = 75$

OMP will be inferior to K-SVD_P at the same sparsity level. By preliminary experiments, we found the optimal T_0 for OMP is around 5. That's to say, once the optimal sparsity level of K-SVD_P drops to lower than 5, it's impossible for OMP to defeat K-SVD_P. Then combined with the optimal sparsity level of K-SVD_P showed in Table 1 and Figure 2, we can draw the conclusion.

4.4. SSIM comparison

Besides PSNR, structural similarity index (SSIM)[30] is included to evaluate. Different from the PSNR, the SSIM is closer to the human visual effect since the correlation between image pixels is considered.

$$\text{SSIM}(\mathbf{x}, \mathbf{y}) = \frac{(2\mu_x\mu_y + C_1)(2\sigma_{xy} + C_2)}{(\mu_x^2 + \mu_y^2 + C_1)(\sigma_x^2 + \sigma_y^2 + C_2)} \quad (11)$$

where μ_x, μ_y are the mean intensity of the discrete signals, and C_1, C_2 are parameters to ensure the stability of SSIM. We use the default parameters and downsampling process.

Table 5 shows the SSIM of OMP and K-SVD_P in $\sigma = 15, 20, 25, 50, 75, 100$. For images Man, House, Lake, Boat, Airplane and Lena which have clear objects in original images, K-SVD_P is almost better than OMP at all noise levels. That is because a similar space in these images leads to high correlations between pixels. For those whose scenes are messy like Map, Bridge and Airport, results are similar to that in PSNR. PSNR is based on error sensitivity but

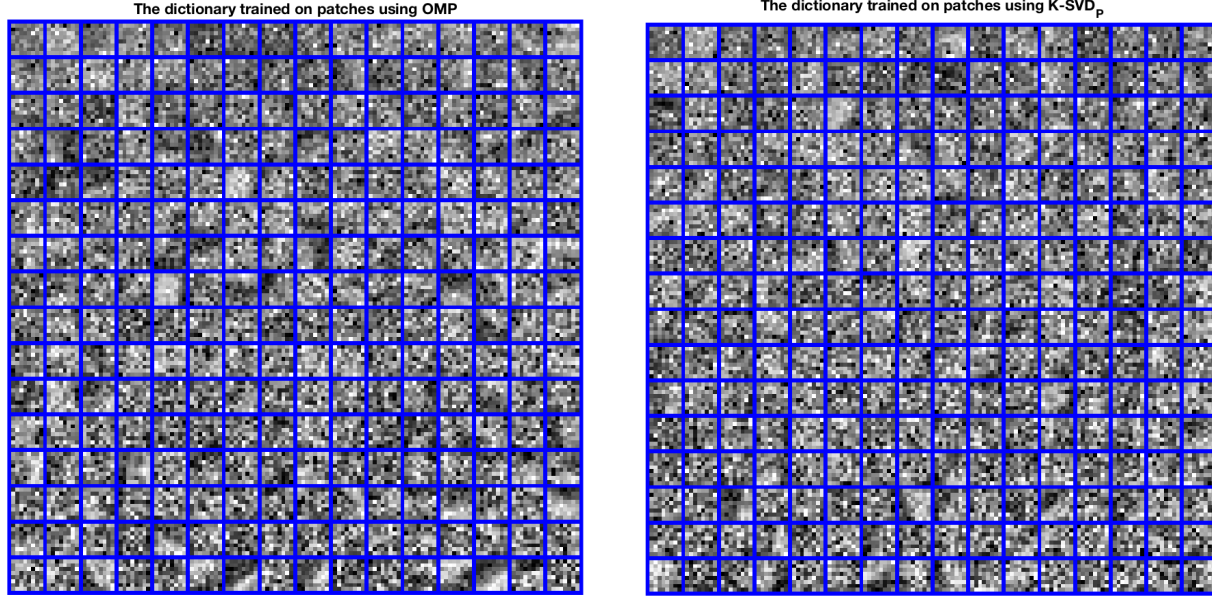
the SSIM perceives image distortion by detecting whether the structural information changes. That's to say, although K-SVD_P is slightly sensitive to error in low noise cases, it managed to maintain a spatial structure which is exactly where human vision is more concerned.

4.5. Visual comparison

Figure 4 and Figure 5 show the denoising details for Lena with $\sigma = 20$ and House with $\sigma = 75$. To some extent, K-SVD_P seems to employ a moving average of the image while OMP is more likely to operate on single points. So when looking at Lena's eye, the OMP processed one is more clear in single points such as eyeballs and eyeliners, while the K-SVD_P operated one has less noise. The House results in $\sigma = 75$ are more obvious. Only the K-SVD_P restores the tail shape though the streaks on it are not clear enough. Figure 6 shows the final adaptive dictionaries trained by Man at $\sigma = 50$. We can see the dictionary obtained by K-SVD_P is highly structured compared to the OMP.

5. Conclusion and Future work

In this paper, we proposed a new K-SVD_P framework equipped with PDAS for sparse representation in image denoising. By introducing the primal-dual variables, the K-SVD_P algorithm directly solves the best subset problem and presents a selection strategy that is different from the



(a) OMP

(b) K-SVD_P

Figure 6. The trianed Dictionary of Man image, $\sigma = 50$

popular greedy algorithms and ℓ_1 optimization. The explicit expression leads to low time complexity, while sufficient KKT condition leads to high accuracy, especially in high noisy cases. Moreover, the experiments demonstrate that the proposal is competitive and feasible compared with two state-of-the-art ways.

The main benefits of our new K-SVD framework are:

- This new framework is superior to BPDN in time complexity and clarity at relatively low noise level;
- In high noise cases, it achieves significantly better performance versus popular OMP algorithm and reduces the time complexity compared to BPDN which makes it possible to utilize;
- Results of SSIM and visual comparisons reveal that it performs better on local patterns.

Future work will include a focus on improving the restoration performance of the K-SVD_P framework at low noise levels and decreasing the time complexity further.

Acknowledgement

This study is supported by NSFC (11801540), Natural Science Foundation of Guangdong (2017A030310572) and Fundamental Research Funds for the Central Universities (WK2040170015, WK2040000016).

References

- [1] A. Abdelhamed, S. Lin, and M. S. Brown. A high-quality denoising dataset for smartphone cameras. In *Proceedings of the IEEE Conference on Computer Vision and Pattern Recognition*, pages 1692–1700, 2018.
- [2] M. Aharon, M. Elad, A. Bruckstein, et al. K-SVD: An algorithm for designing overcomplete dictionaries for sparse representation. *IEEE Transactions on signal processing*, 54(11):4311, 2006.
- [3] G. Baloch and H. Ozkaramanli. Image denoising via correlation-based sparse representation. *Signal, Image and Video Processing*, 11(8):1501–1508, 2017.
- [4] F. Bergeaud and S. Mallat. Matching pursuit of images. In *Proceedings., International Conference on Image Processing*, volume 1, pages 53–56. IEEE, 1995.
- [5] S. S. Chen, D. L. Donoho, and M. A. Saunders. Atomic decomposition by basis pursuit. *SIAM review*, 43(1):129–159, 2001.
- [6] Y. Chen. Fast dictionary learning for noise attenuation of multidimensional seismic data. *Geophysical Journal International*, 209(1):21–31, 2017.
- [7] W. Dong, L. Zhang, G. Shi, and X. Li. Nonlocally centralized sparse representation for image restoration. *IEEE transactions on Image Processing*, 22(4):1620–1630, 2013.
- [8] B. Efron, T. Hastie, I. Johnstone, R. Tibshirani, et al. Least angle regression. *The Annals of statistics*, 32(2):407–499, 2004.
- [9] M. Elad and M. Aharon. Image denoising via sparse and redundant representations over learned dictionaries. *IEEE Transactions on Image processing*, 15(12):3736–3745, 2006.

- [10] Q. Guo, C. Zhang, Y. Zhang, and H. Liu. An efficient SVD-based method for image denoising. *IEEE transactions on Circuits and Systems for Video Technology*, 26(5):868–880, 2016.
- [11] T. Hastie, R. Tibshirani, and R. J. Tibshirani. Extended comparisons of best subset selection, forward stepwise selection, and the lasso. *arXiv preprint arXiv:1707.08692*, 2017.
- [12] K. Ito and K. Kunisch. A variational approach to sparsity optimization based on Lagrange multiplier theory. *Inverse problems*, 30(1):015001, 2013.
- [13] J.-W. Jhang and Y.-H. Huang. A high-SNR projection-based atom selection OMP processor for compressive sensing. *IEEE Transactions on Very Large Scale Integration (VLSI) Systems*, 24(12):3477–3488, 2016.
- [14] Y. Liu, S. Canu, P. Honeine, and S. Ruan. Mixed Integer Programming for Sparse Coding: Application to Image Denoising. *IEEE Transactions on Computational Imaging*, 2019.
- [15] X. Lu and X. Lü. ADMM for image restoration based on nonlocal simultaneous sparse Bayesian coding. *Signal Processing: Image Communication*, 70:157–173, 2019.
- [16] B. K. Natarajan. Sparse approximate solutions to linear systems. *SIAM journal on computing*, 24(2):227–234, 1995.
- [17] B. A. Olshausen and D. J. Field. Sparse coding with an over-complete basis set: A strategy employed by v1? *Vision research*, 37(23):3311–3325, 1997.
- [18] T. Plotz and S. Roth. Benchmarking denoising algorithms with real photographs. In *Proceedings of the IEEE Conference on Computer Vision and Pattern Recognition*, pages 1586–1595, 2017.
- [19] M. Protter and M. Elad. Image sequence denoising via sparse and redundant representations. *IEEE Transactions on Image Processing*, 18(1):27–35, 2009.
- [20] J. Qian, T. Hastie, J. Friedman, R. Tibshirani, and N. Simon. Glmnet for matlab. *Accessed: Nov, 13:2017–2017*, 2013.
- [21] M. E. R. Rubinstein, A. M. Bruckstein. Dictionaries for sparse representation modeling. *IEEE Proc.*, 98(6):1045–1057, June 2010.
- [22] S. Rosset and J. Zhu. Piecewise linear regularized solution paths. *The Annals of Statistics*, pages 1012–1030, 2007.
- [23] R. Rubinstein, A. M. Bruckstein, and M. Elad. Dictionaries for sparse representation modeling. *Proceedings of the IEEE*, 98(6):1045–1057, 2010.
- [24] M. Sajjad, I. Mehmood, N. Abbas, and S. W. Baik. Basis pursuit denoising-based image superresolution using a redundant set of atoms. *Signal, Image and Video Processing*, 10(1):181–188, 2016.
- [25] K. Sjöstrand, L. H. Clemmensen, R. Larsen, G. Einarsson, and B. K. Ersbøll. Spasm: A matlab toolbox for sparse statistical modeling. *Journal of Statistical Software*, 84(10), 2018.
- [26] J. Sulam, B. Ophir, and M. Elad. Image denoising through multi-scale learnt dictionaries. In *2014 IEEE International Conference on Image Processing (ICIP)*, pages 808–812. IEEE, 2014.
- [27] R. Tibshirani. Regression shrinkage and selection via the lasso. *Journal of the Royal Statistical Society: Series B (Methodological)*, 58(1):267–288, 1996.
- [28] J. A. Tropp. Greed is good: Algorithmic results for sparse approximation. *IEEE Transactions on Information theory*, 50(10):2231–2242, 2004.
- [29] J. A. Tropp and A. C. Gilbert. Signal recovery from random measurements via orthogonal matching pursuit. *IEEE Transactions on information theory*, 53(12):4655–4666, 2007.
- [30] Z. Wang, A. C. Bovik, H. R. Sheikh, E. P. Simoncelli, et al. Image quality assessment: from error visibility to structural similarity. *IEEE transactions on image processing*, 13(4):600–612, 2004.
- [31] C. Wen, A. Zhang, S. Quan, and X. Wang. Bess: An R Package for Best Subset Selection in Linear, Logistic and CoxPH Models. *arXiv preprint arXiv:1709.06254*, 2017.
- [32] H. Zou. The adaptive lasso and its oracle properties. *Journal of the American statistical association*, 101(476):1418–1429, 2006.